



Metamaterial Structure Effect on Printed Antenna for LTE/WIFI /Cancer Diagnosis

Fatma Taher¹, A. M. M. A. Allam², Ahmed F. Miligy³, Mohamed A. Mohamed^{4,5}, Mohamed Fathy Abo Sree^{6,*}, Sara Yehia Abdel Fatah^{7,8}

- ¹ College of Technological Innovation, Zayed University, P.O. Box 19282, Dubai, UAE
- ² Department of Communication and Electronics, Arab Academy for Science, Technology and Maritime Transport, Cairo, Egypt
- ³ Air Defence College Alexandria University, Alexandria, Egypt
- ⁴ Department of Electronics and Communications Engineering, Faculty of Engineering, Ahram Candian University, Cairo, Egypt
- ⁵ Department of Communication and Electronics, Arab Academy for Science, Technology and Maritime Transport, Cairo, Egypt
- ⁶ Department of Electronics and Communications Engineering, Arab Academy for Science, Technology and Maritime Transport, Cairo 451913, Egypt
- ⁷ Department of Mechatronics Engineering and Automation, Faculty of Engineering, Egyptian Chinese University, Cairo, Egypt
- ⁸ Higher Institute of Engineering and Technology, EL-Tagmoe EL-Khames, New Cairo, Egypt

ARTICLE INFO

Article history:

Received 13 October 2023
Received in revised form 22 January 2024
Accepted 2 May 2024
Available online 22 May 2024

Keywords:

Metamaterial antenna, Printed antenna, LTE application, Cancer Diagnosis

ABSTRACT

This paper explores the influence of metamaterial structures on the performance of LTE/Wi-Fi printed antennas, examining two antenna versions. One version integrates a metamaterial ground layer, representing the traditional antenna, while the other incorporates a metamaterial load attached to the modified antenna. The inclusion of the metamaterial ground layer supports the unit cell with the MTM structure, enabling an analysis of how the MTM structure impacts antenna performance. Testing is conducted using Roger 5880 substrate with a thickness of 1.575 mm and a dielectric constant of 2.2. The antenna's overall dimensions are 60×49×1.575mm, with a loss tangent of 0.0009. Once optimal inductor/capacitor values are determined, equivalent circuits are generated for both the planned and conventional circuits. These circuits are simulated using CST Microwave Studio, with the Path Wave ADS simulator running the equivalent circuit. Antenna manufacturing and measurement are conducted using a Network Analyzer. Frequency ranges covered by the antenna include 1.68 GHz to 2.51 GHz, 3.56 GHz to 4.63 GHz, and 4.1 GHz to 5.1 GHz, suitable for standard applications. Simulated gain is reported as 2.58 dB/2.45 dB, with observed gain at 2.22 dB/5.19 dB, showing excellent agreement between measured and simulated values from both simulators. Additionally, simulated specific absorption rate (SAR) on a sample Breast Phantom ensures compliance with the 1g/10g SAR value requirements set by the European Union and the United States. This confirms the antenna's suitability for cancer diagnosis and detection applications

1. Introduction

* Corresponding author.

E-mail address: Dr.eng.m.fathy2019@hotmail.com

<https://doi.org/10.37934/araset.46.1.237249>

The path wave ADS simulator runs the equivalent circuit. The antenna Rode is manufactured and measured by Network Analyzer. The frequency ranges covered by the antenna are as follows: 1.68 GHz-2.51 GHz 3.56-4.63 GHz 4.1 GHz-5.1 GHz Standard applications (LTE, Wi-Fi, etc.) 2.58dB/2.45dB. However, printed thin strip antennas have become necessary for every new gadget due to the explosive proliferation of handheld wireless communication devices in the previous several years. This sort is good since it achieves the smallest size and covers all of the frequency ranges required in today's different applications. Users and service providers frequently want wireless devices with antennas that are tiny and compact, easy to link with other components of a wireless communication system, low profile, and reasonably priced to manufacture, in addition to meeting operational criteria [7–10].

However, compared to devices and bodies, flexible or thinner substrate-based wearable antennas provide a number of benefits, one of which is the ability to design simpler configurations. They can also include gates in a variety of shapes, such as bodies or gadgets [11–15]. They can also be supported by MTM cells, which can increase gain and bandwidth [18–19].

Regarding MTM, it is a substance that is usually synthesized with unique or artificial structures in order to generate electromagnetic characteristics that are uncommon or challenging to generate in the natural world. It is abnormal and has distinct qualities that aren't found in the natural environment [20–21]. It has a negative permeability, a negative dielectric constant, or both [22]. Many people are interested in them because of their features, and they may find utility in a wide range of electromagnetic applications, from the microwave to the optical regime [22–26].

This report provides a thorough analysis of the most recent research initiatives related to those MTM-based tiny antennas. They are analyzed and classified into multiple kinds, including MTM loadings, metaresonators, and antennas based on dispersion engineering. A few real-world obstacles or restrictions on the advancement of MTM-based tiny antennas are mentioned, along with potential solutions.

Another significant occurrence that is happening increasingly frequently these days is the diagnosis of breast cancer. It is a contributing factor to the greatest annual number of women's cancer cases that are reported. In Malaysia, women are more likely than men to have cancer; in 2016, 10,290 cases out of 100,000 individuals had the highest incidence (14.5%), according to [27]. This is in contrast to other cancer cases, such as leukaemia, stomach, and lung cancer. Unchecked aberrant cell development produces malignant tumours, which are usually referred to as cancer. These tumours can move to other organs or infect surrounding body components. It is imperative to identify a diagnosis and a means of detection for this illness.

Antennas placed within or on top of bodily organs can be used to detect cancer. Additionally, while researching and using an implanted antenna for the detection of human cancer, SAR presents a safety risk [28–40]. After fabrication, the antennas are measured. Similar circuit technology is also used to test it, producing the ideal conductor and capacitor values [41-44].

2. Methodology

2.1 Antenna Design

2.1.1 Conventional antenna

A typical patch antenna is shown in Figure 1. This study presents a microstrip antenna design with and without MTM. Applications for WiFi and LTE use it. Studies on the human breast are being conducted concurrently to determine whether or not it could be utilized as a sensor for the identification and diagnosis of cancer. The patch combines multiple horizontal strips to partially realise the LTE frequency spectrum. Its measurements are shown in Table I, and the manufactured

version is shown in Figure 2. Based on Roger 5880, the design has a thickness of 1.575 mm and a ϵ_r of 2.2.

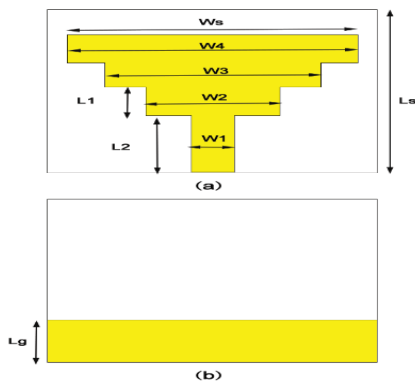


Fig. 1. Conventional Antenna Structure: (a) Top View, (b) Bottom View

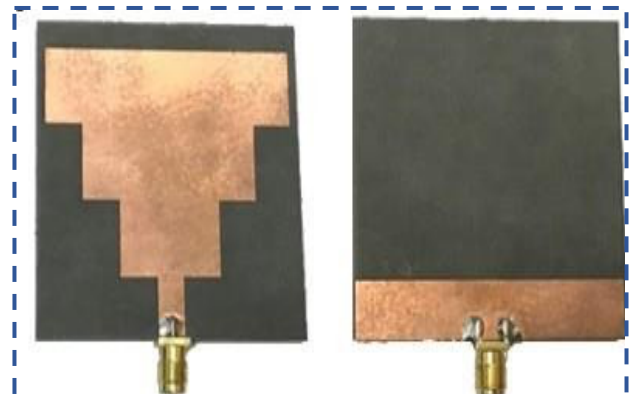


Fig. 2. Conventional Antenna Fabrication: (a) Top View, (b) Bottom View

Table 1
 Reconfigurable-Pin Diode Switches

| Antenna Parameter | Dimension(mm) |
|-------------------|------------------|
| w _s | 49 |
| w ₁ | 4.80 |
| w ₂ | 20 |
| w ₃ | 30 |
| w ₄ | 48 |
| l _s | 60 |
| l ₁ | 12 |
| l ₂ | 11 |
| W _p | 14 |
| L _g | 8(conv.),11(MTM) |

Figure 3 illustrates the model of the structure's similar circuit. It is made up of three inductors, three capacitors, and a resistor that mimics the resistance of the patch. The values of these components are found using equations 1 and 2, where l is the length of the strip, w is its width, h is the height of the substrate, and c is the speed of light in vacuum.

$$L = 0.000508 l \left[\ln\left(\frac{2l}{w+h}\right) + 0.5 + 0.2235\left(\frac{w+h}{l}\right) \right] \quad (1)$$

$$C = \frac{\epsilon_r l \left[\frac{w}{h} + 1.393 + 0.667 \ln\left(\frac{w}{h} + 1.444 \right) \right]}{120\pi c} \quad (2)$$

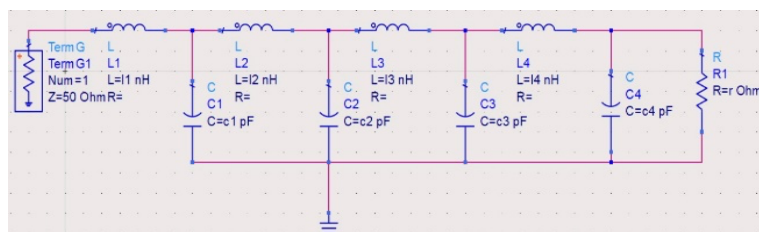


Fig. 3. Equivalent circuit of conventional antenna.

2.1.2 Metamaterial Antenna

The built MTM antenna is depicted in Figure 5, its equivalent circuit is illustrated in Figure 6, and the bottom layer of DGS ground is substituted with a layer composed of a 3x3 array of copper patches spaced 1.00 mm apart. Table I displays its measurements.

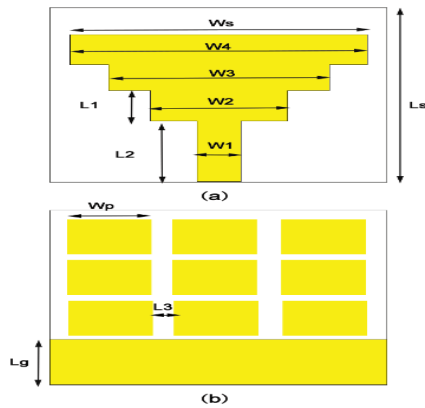


Fig. 4. MTM Antenna Structure: (a) Top View, (b) Bottom View

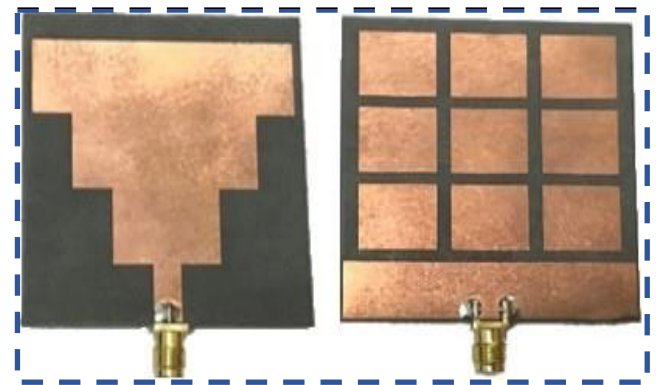


Fig. 5. MTM Antenna Fabrication: (a) Top View (b) Bottom View

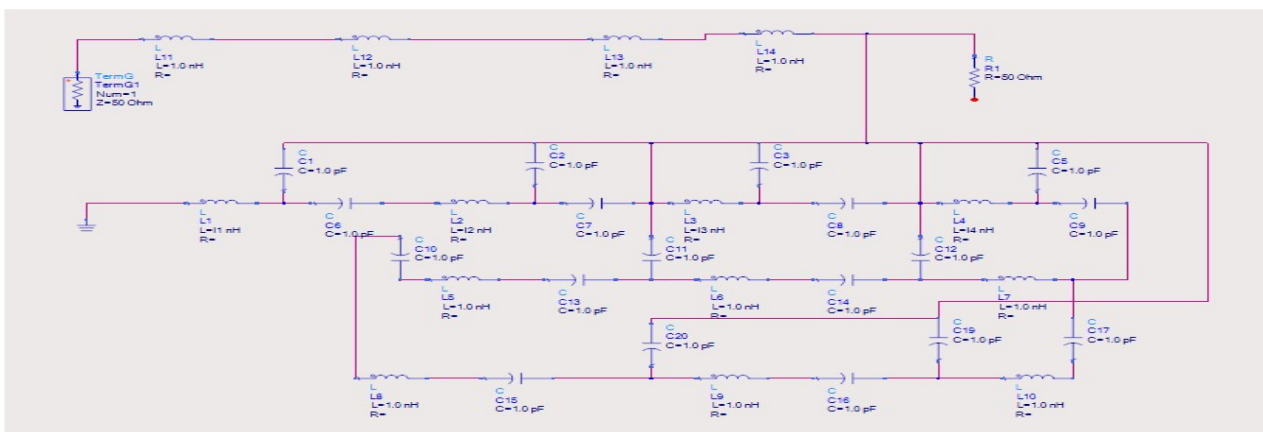


Fig. 6. Equivalent circuit of MTM antenna

2.2 Optimization

The goal of this part is to optimise the two antennas' various dimensions in order to reach the targeted frequency ranges of 2.1 GHz and 4.1 GHz.

2.2.1 Conventional Antenna

The optimization of a standard antenna's size to reach resonance frequencies of 2.1 GHz and 4.1 GHz is illustrated in Figure 7. As seen in figures 7a, b, and c, respectively, the reflection coefficient is optimized for various values of substrate thickness (h_s), patch width (W_4), and ground length (l_g).

It is evident that the primary element affecting the second response at 4.1 GHz is the ground length (l_g), with an optimal value of 10mm. It is evident that modifications to the dielectric thickness

(hs) and patch width (w1) can induce resonance at 2.1 GHz, whereas ground length modifications can induce resonance at 4.1 GHz.

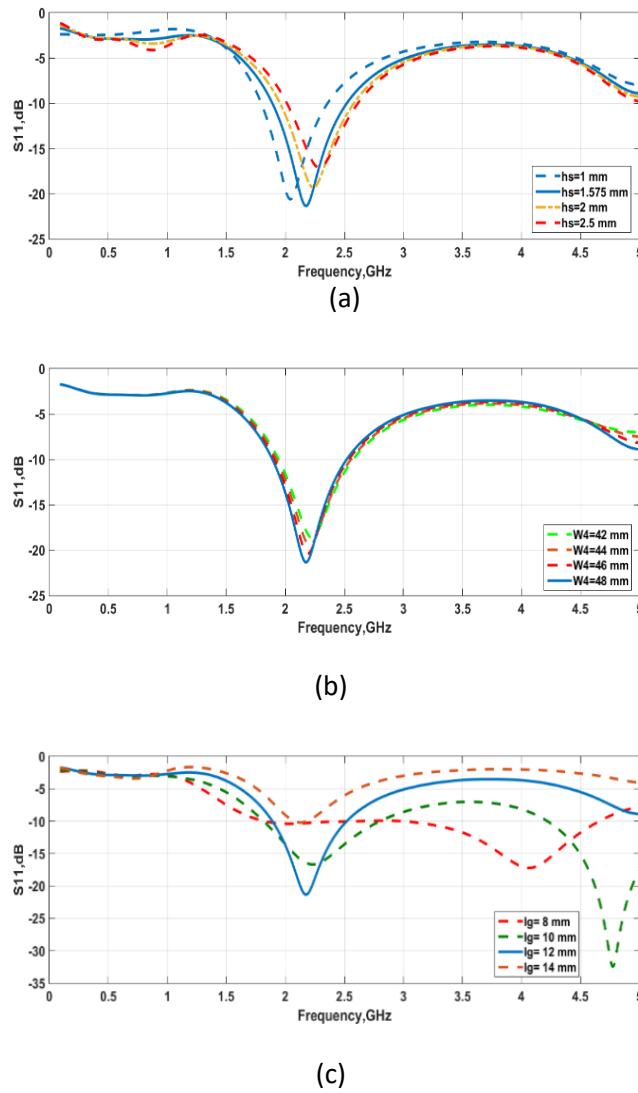


Fig. 7. conventional antenna optimization (a) substrate thickness, (b) patch width and (c) ground length

The simulated and measured reflection coefficient of the optimized conventional antenna is presented in Figure 8, and the findings are in good agreement with the simulations.

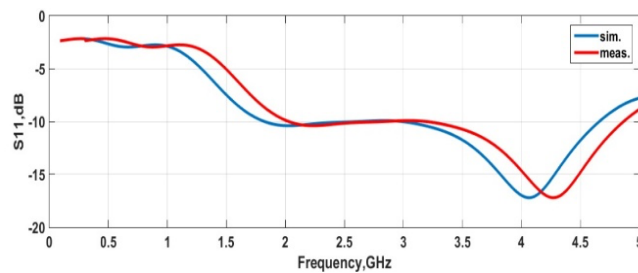


Fig. 8. Simulated and measured of the reflection coefficient of the optimized conventional antenna

2.2.2 MTM Antenna

The reflection coefficient for a range of unit cell edges (w_p) optimized to reach both 2.1 GHz and 4.1 GHz resonance frequencies is displayed in Figure 9. It is evident that the ideal unit cell square edge (w_p) value is 14 mm since both resonances are apparent.

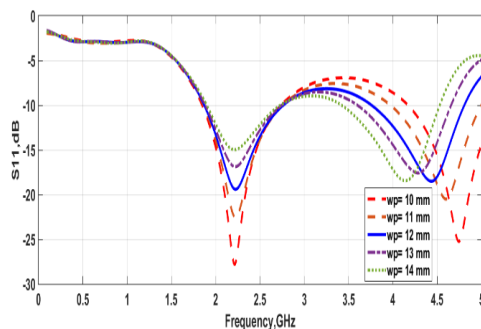


Fig. 9. MTM's unit cell edge antenna optimization

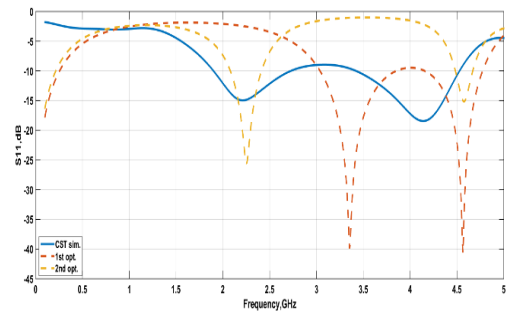


Fig. 10. MTM equivalent circuit optimization

Starting with initial values of 1nH and 1pF, respectively, Figure 10 illustrates the equivalent circuit response of the MTM antenna for various parametric adjustments for the values of capacitors and inductors. It is evident that optimization number two is capable of reaching both 2.1GHz and 4.1GHz (2).

3. Results

3.1 Return losses and Gain

Figure 11 shows the optimized MTM antenna's simulated and observed reflection coefficients, showing a high agreement between them.

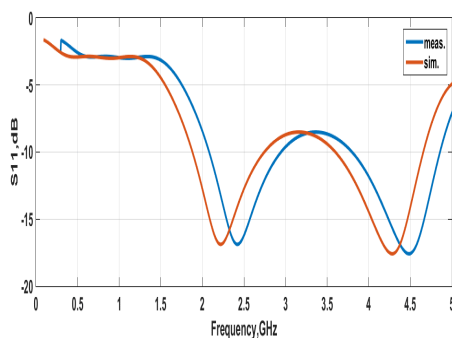


Fig. 11. MTM equivalent circuit optimization

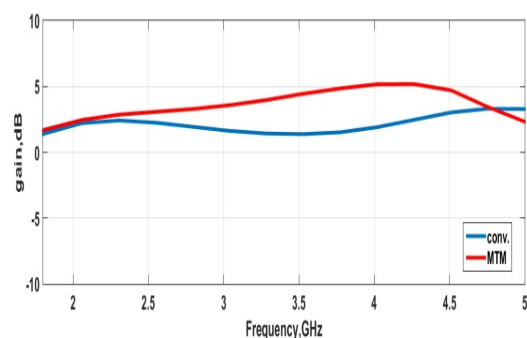


Fig. 12. MTM equivalent circuit optimization

Fig 12 presents the conventional antenna's gain versus the MTM one. One can observe that the MTM's gain is slightly increased.

3.2 Radiation Pattern

Figure 13 shows the 3D radiation pattern for the conventional antenna operating at 4.1 GHz and with a gain of 4.29 dB. Figure 14 shows the 2D radiation pattern in the XZ and YZ planes.

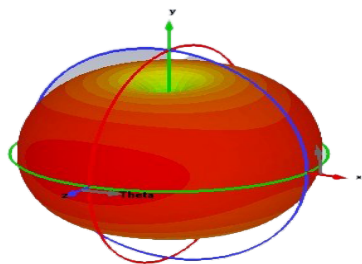


Fig. 13. 3D radiation pattern of conventional antenna at 4.1 GHz

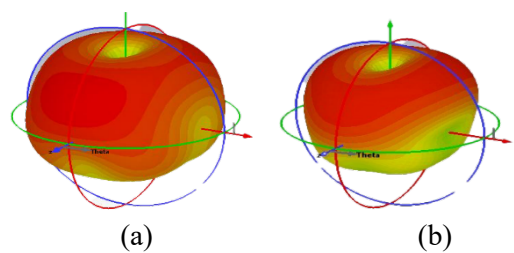
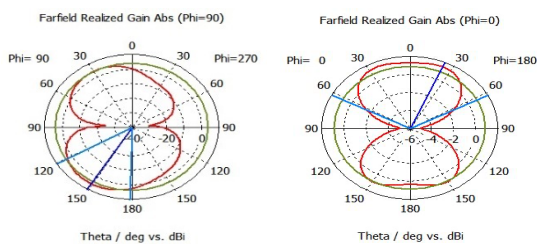
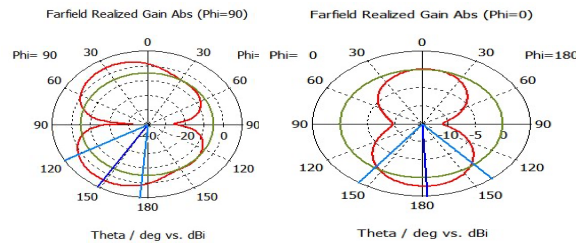


Fig. 15. 3D radiation pattern of MTM antenna: (a) at 2.1GHz, (b) at 4.1GHz



(a) XZ Plane (b) XY Plane

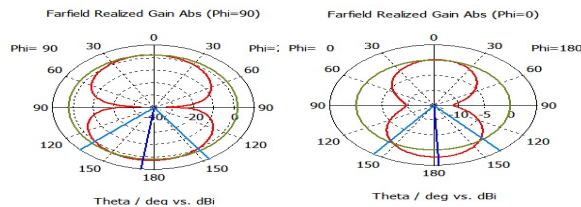
Fig. 14. 2D radiation pattern of conventional pattern at 4.1 GHz



(a) XZ Plane (b) XY Plane

Fig. 16. 2D radiation pattern of MTM antenna at 2.1 GHz (a) XZ plane, (b)YZ plane

At 2.1 GHz and 4.1 GHz, Figure 15 shows the 3D radiation pattern of the MTM antenna. The measured gains are 2.22 dB and 5.19 dB, while the simulated gains are 2.58 dB and 5.45 dB, respectively. The 2D radiation pattern in the XZ and YZ planes for the same frequency is shown in Figures 16 and 17.



(a) XZ Plane (b) XY Plane

Fig. 17. 2D radiation pattern of MTM antenna at 4.1 GHz (a) XZ plane, (b)YZ plane

3.3 Surface Current

A typical 2.1GHz antenna's surface current is shown in Figure 18, with higher values at the edges. The MTM antenna's surface current is shown in Figure 19 for frequencies of 2.1 and 4.1 GHz, respectively.

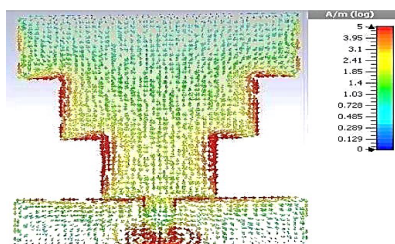


Fig. 18. surface current for conventional antenna at 2.1GHz

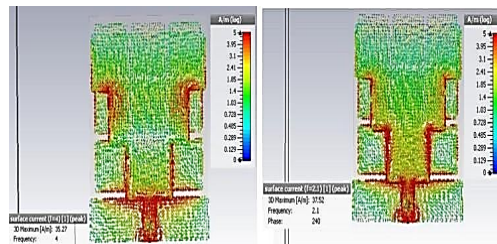


Fig. 19. Surface current for MTM antenna at:(a) 2.1 GHz, (b) 4.1 GHz

3.4 Antenna Performance on Body

The next investigation will use a phantom breast to assess the efficacy of the proposed antenna design. CST is applied to 1 and 10 grammes in numerical research. To replicate the anatomy of the human breast, a multilayer model tissue has been constructed.

3.4.1 SAR evaluation

The safety of the antenna operating over a human body was evaluated in order to make sure the SAR level complied with safety regulations. The FCC and ICNIRP's regulatory recommendations, which set a maximum level of 1.6 W/kg for averages over 1 gramme of tissue and 2 W/kg for averages over 10 grammes of tissue, form the basis of the evaluation. The SAR evaluation employed the CST standard with a 100 mW input power. In order to replicate the human anatomy, both antennas are used in this experiment on a layered human breast. CST is used for numerical analysis on 1g and 10g samples.

Generally, the model was 10 mm away from the design while evaluating it along the x-axis. For the conventional antenna (Figures 20 and 21) and the MTM antenna (Figures 22 and 23), the findings are shown in Tables II and III, respectively. When compared to the standards, the results are satisfactory. Tables 2 and 3 show the SAR findings for the conventional and MTM antennas, respectively.

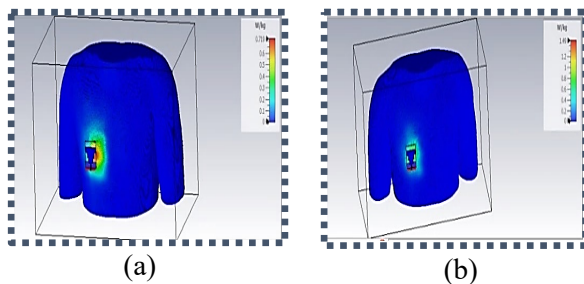


Fig. 20. SAR analysis of conv. antenna at 2GHz (a) 10g ,(b) 1g

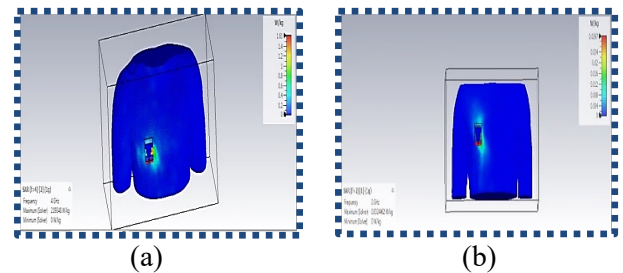


Fig. 22. SAR analysis of MTM antenna at 2GHz (a) 10g, (b) 1g

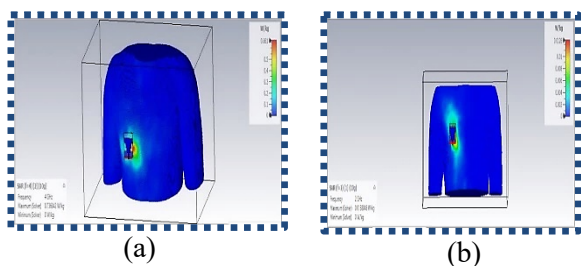


Fig. 21. SAR analysis of conv. antenna at 4GHz (a) 10g, (b) 1g

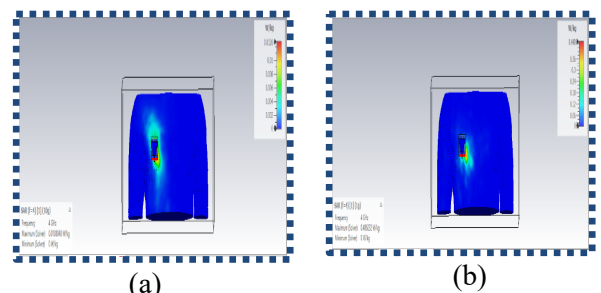


Fig. 23. SAR analysis of MTM antenna at 4GHz (a) 10g, (b) 1g

Figures 23 and 24 display the SAR values for an MTM antenna, while Figure 22 displays the SAR values in the breast for a traditional antenna operating at 4.1 GHz. The results for each antenna are summarized in Tables 2 and 3.

Table 2
 SAR analysis of conventional antenna Values near breast

| SAR (10 mm in distance from breast) | SAR at 1(g) W/Kg | SAR at 10(g) W/Kg |
|-------------------------------------|------------------|-------------------|
| At 2 GHz | 1.49 | 0.719 |
| At 4 GHz | 1.61 | 0.66 |

Table 3
 SAR analysis of MTM antenna Values near breast

| SAR (10 mm in distance from breast) | SAR at 1(g) W/Kg | SAR at 10(g) W/Kg |
|-------------------------------------|------------------|-------------------|
| At 2 GHz | .029 | .0126 |
| At 4 GHz | .448 | 0.105 |

Table 4 compares different planar metasurface-transistor (MTM) antenna designs found in the literature to accepted work.

Table 4
 Summary of research on planar MTM / metasurface structure-based antennas

| First author, year | Substrate material | Dimensions @ Array | Frequency | antenna Efficiency Simulated |
|--------------------------------|--------------------------------|---------------------------------|-------------------------|------------------------------|
| H.T. Zhong, 2017 [40] | Rogers RT5880 | Duroid 0.6λ0 | 5.4 GHz | 92% at 0° |
| Wei Hu, 2019 [41] | F4B/air | @ 3×3 unit cells | 2.45 GHz | 98% at 60° |
| Omar M. | Rogers RT5880 | Duroid 0.6λ0 | 5.8 GHz | (TM-mode) |
| Ramahi, 2012 [42] | Rogers RT5880 | Duroid @ 8×8 unit cells | 5.55 GHz | 87.6% |
| Babak Alavikia, 2015 [43] | Rogers RO4003 | Approximately 0.114λ0 | 5.6 GHz | - |
| Babak Alavikia 2015 [44] | F4B | @ 9×9 unit cells | 2.5 GHz (LTE/Wi-Fi) | 92% for G- CSRR |
| Xuanming Zhang 2018 [45] | Rogers TMM10i | 0.34λ0 | 3 GHz | 87% |
| | Rogers RO3010 PCB | @ 11×11 array of G-CSRR and 5×5 | 5.33 GHz (WiFi) | 90% |
| Thamer S. | Polytetrafluoroethylene (PTFE) | array microstrip patch antenna | 2.45 GHz | 97% |
| Almoneef 2015 [46] | - | Approximately | 5.8 GHz | 86% |
| Alireza Ghaneizadeh, 2019 [47] | Rogers RT/duroid 6006 | λ0/5 | 2.45 GHz and 6 GHz | 99.5% |
| Xin Duan, 2018 [48] | F4B | @ 9×9 unit cells | 900 MHz, | 88% at 0° and |
| | F4B-2 | Approximately 0.131λ0 | 2.6 GHz and | 77% at 75° |
| Fan Yu, 2018 [49] | Rogers RO4003 | @ 9×9 unit cells | 5.7 GHz | Higher than 90% |
| B. Ghaderi, 2018 [50] | Roger 5880 | 0.075λ0 | Wideband (6.2–21.4 GHz) | 70%, 80%, |
| Xuanming Zhang, 2017 [51] | Rogers RT5880 | Duroid @ 13×13 unit cells | 1.75 GHz, | and 82% at |
| H.T. Zhong, 2017 [52] | F4B/air | 0.13λ0 | 3.8 GHz, and | 900 MHz, 2.6 |
| H.T. Zhong, 2016 [53] | Rogers RT5880 | Duroid @ 11×11 unit cells | 5.4 GHz | GHz and 5.7 GHz, |
| This work | Rogers RT5880 | Duroid 0.16λ0 | 2.1 GHz and | respectively |

Table 4 shows that, in comparison to previous efforts, the antenna efficiency is 94% over the two operating bands.

4. Conclusions

This study presents, analyses, fabricates, and measures conventional and MTM LTE/Wi-Fi/disease diagnostic antennas. Both CST and ADS simulators are used to build models of the two antennas. There is good agreement between the calculated and measured reflection coefficients. The MTM version conducts resonance at 2.1 GHz and a gain of 5.45 dB at 4.1 GHz with a bandwidth of 1.07 GHz, and a bandwidth of 0.832 GHz with a gain of 2.58 dB. In contrast, the conventional antenna operates at 4.1 GHz with a bandwidth of 1.65 GHz and a gain of 4.29 dB.

References

- [1] Syed, Abdul Basit. "Dimensioning of LTE Network." Master's thesis, Helsinki University of Technology, 2009.
- [2] Elsadek, Hala A., Esmat A. Abdallah, Dalia M. Elsheakh, and Heba Badr El-Din El-Shaarawy. "Microstrip antennas: Future trends and new applications." *International Journal of Antennas and Propagation* 2013 (2013). <https://doi.org/10.1155/2013/890764>
- [3] Roshan, Rakesh, Seetaram Prajapati, Harshita Tiwari, and Greeshmaja Govind. "A dual wideband monopole antenna for GSM/UMTS/LTE/WiFi/and lower UWB application." In *2018 3rd International Conference on Microwave and Photonics (ICMAP)*, pp. 1-2. IEEE, 2018. <https://doi.org/10.1109/ICMAP.2018.8354635>
- [4] Bashri, M. S. R., Tughrul Arslan, and Wei Zhou. "A dual-band linear phased array antenna for WiFi and LTE mobile applications." In *2015 Loughborough Antennas & Propagation Conference (LAPC)*, pp. 1-5. IEEE, 2015. <https://doi.org/10.1109/LAPC.2015.7366010>
- [5] Zhu, Yuan, Min Quan Li, and Hong Qing He. "A compact dual-band monopole antenna for 4G LTE and WIFI utilizations." In *2016 IEEE MTT-S International Microwave Workshop Series on Advanced Materials and Processes for RF and THz Applications (IMWS-AMP)*, pp. 1-4. IEEE, 2016.
- [6] Kumari, Anjali, and Ritesh Kumar Badhai. "A dual-band high-gain base-station antenna for WLAN and Wi-MAX applications." In *2017 International Conference on Innovations in Information, Embedded and Communication Systems (ICIIECS)*, pp. 1-4. IEEE, 2017. <https://doi.org/10.1109/ICIIECS.2017.8275871>
- [7] Ibrahim, Muhammad Aly, W. Swelam, Abd El-Azeem, H. Mohamed, and Hadia El Hennawy. "Ultra-wide band microstrip antenna for 4G applications." In *International Conference on Aerospace Sciences and Aviation Technology*, vol. 18, no. 18, pp. 1-9. The Military Technical College, 2019.
- [8] Fatah, Sara Yehia Abdel, Ehab KIKI Hamad, Wael Swelam, A. M. M. A. Allam, Mohamed Fathy Abo Sree, and Hesham A. Mohamed. "Design and implementation of UWB slot-loaded printed antenna for microwave and millimeter wave applications." *IEEE Access* 9 (2021): 29555-29564. <https://doi.org/10.1109/ACCESS.2021.3057941>
- [9] Taher, F., Ahmed Shokry Tonsy, Hesham Hanafy MT Azab, Hussam Al Hamadi, Mohammad T. Haweel, and Mohamed Fathy Abo Sree. "Design and implementation of 2.6 GHz Phase shift using microstrip technology for mobile broadband application." In *2022 International Telecommunications Conference (ITC-Egypt)*, pp. 1-7. IEEE, 2022. <https://doi.org/10.1109/ITC-Egypt5520.2022.9855749>
- [10] Louertani, Karim, Ruifeng Huang, and Tan-Huat Chio. "Wideband and low-profile unidirectional spiral antenna with Meta-material absorber." In *2013 IEEE Antennas and Propagation Society International Symposium (APSURSI)*, pp. 682-683. IEEE, 2013. <https://doi.org/10.1109/APS.2013.6711001>
- [11] Abdel-Rahman, Adel B., and Ahmed A. Ibrahim. "Gain enhancement of aperture coupled patch antenna using metamaterial and conical metal frame." In *The 2nd Middle East Conference on Antennas and Propagation*, pp. 1-5. IEEE, 2012. <https://doi.org/10.1109/MECAP.2012.6618196>
- [12] S. Genovesi, F. Costa, and G. Manara, "Compact antenna for wearable applications," in Proc. 2nd URSI Atlantic Radio Sci. Meeting (AT-RASC), May 2018, pp. 1–3. <https://doi.org/10.23919/URSI-AT-RASC.2018.8471491>
- [13] Ashap, Adel YI, Z. Z. Abidin, S. H. Dahlan, H. A. Majid, S. K. Yee, Gameel Saleh, and Norun Abdul Malek. "Flexible wearable antenna on electromagnetic band gap using PDMS substrate." *TELKOMNIKA (Telecommunication Computing Electronics and Control)* 15, no. 3 (2017): 1454-1460. <https://doi.org/10.12928/telkomnika.v15i3.7214>
- [14] Seman, Fauziahanim Che, Faisal Ramadhan, Nurul Syafeeqa Ishak, Rudy Yuwono, Zuhairiah Zainal Abidin, Samsul Haimi Dahlan, Shaharil Modd Shah, and Adel Yahya Isa Ashyap. "Performance evaluation of a star-shaped patch antenna on polyimide film under various bending conditions for wearable applications." *Progress In Electromagnetics Research Letters* 85 (2019): 125-130. <https://doi.org/10.2528/PIERL19022102>

- [15] Ashyap, Adel YI, Wan Noor Najwa Wan Marzudi, Zuhairiah Zainal Abidin, Samsul Haimi Dahlan, Huda A. Majid, and Muhammad Ramlee Kamaruddin. "Antenna incorporated with Electromagnetic Bandgap (EBG) for wearable application at 2.4 GHz wireless bands." In *2016 IEEE Asia-Pacific Conference on Applied Electromagnetics (APACE)*, pp. 217-221. IEEE, 2016. <https://doi.org/10.1109/APACE.2016.7915890>
- [16] Muhammad, Zuraidah, S. M. Shah, Z. Z. Abidin, Adel YI Asyhap, S. M. Mustam, and Y. Ma. "CPW-fed wearable antenna at 2.4 GHz ISM band." In *AIP Conference Proceedings*, vol. 1883, no. 1. AIP Publishing, 2017. <https://doi.org/10.1063/1.5002021>
- [17] Gao, Guo-Ping, Chen Yang, Bin Hu, Rui-Feng Zhang, and Shao-Fei Wang. "A wide-bandwidth wearable all-textile PIFA with dual resonance modes for 5 GHz WLAN applications." *IEEE Transactions on Antennas and Propagation* 67, no. 6 (2019): 4206-4211. <https://doi.org/10.1109/TAP.2019.2905976>
- [18] Pendry, John B., A. J. Holden, D. J. Robbins, and W. J. Stewart. "Low frequency plasmons in thin-wire structures." *Journal of Physics: Condensed Matter* 10, no. 22 (1998): 4785. <https://doi.org/10.1088/0953-8984/10/22/007>
- [19] Pendry, John B., Anthony J. Holden, David J. Robbins, and W. J. Stewart. "Magnetism from conductors and enhanced nonlinear phenomena." *IEEE transactions on microwave theory and techniques* 47, no. 11 (1999): 2075-2084. <https://doi.org/10.1109/22.798002>
- [20] He, Yingran, Sailing He, and Xiaodong Yang. "Optical field enhancement in nanoscale slot waveguides of hyperbolic metamaterials." *Optics Letters* 37, no. 14 (2012): 2907-2909. <https://doi.org/10.1364/OL.37.002907>
- [21] Baviskar, Jaypal, Vikram Singh, and Amutha Jeyakumar. "Meta-material embedded designing of 2.4 GHz patch array antenna for wireless communication." In *2015 International Conference on Communication, Information & Computing Technology (ICCICT)*, pp. 1-6. IEEE, 2015. <https://doi.org/10.1109/ICCICT.2015.7045721>
- [22] Luo, Shengyuan, Yingsong Li, and Wanlu Shi. "A dual-frequency antenna array with mutual coupling reduction via metamaterial structures." In *2018 IEEE International Symposium on Antennas and Propagation & USNC/URSI National Radio Science Meeting*, pp. 1385-1386. IEEE, 2018. <https://doi.org/10.1109/APUSNCURSINRSM.2018.8609399>
- [23] Pajovic, M., Z. Potocnik, and V. Djeric. "Dual band metamaterial-structured antenna with coplanar waveguides and radial feed stub." In *2015 IEEE International Symposium on Antennas and Propagation & USNC/URSI National Radio Science Meeting*, pp. 822-823. IEEE, 2015. <https://doi.org/10.1109/APS.2015.7304798>
- [24] Yu, Kai, Xiaoguang Liu, and Yingsong Li. "Mutual coupling reduction of microstrip patch antenna array using modified split ring resonator metamaterial structures." In *2017 IEEE International Symposium on Antennas and Propagation & USNC/URSI National Radio Science Meeting*, pp. 2287-2288. IEEE, 2017. <https://doi.org/10.1109/APUSNCURSINRSM.2017.8073186>
- [25] Li, Ke, Cheng Zhu, Long Li, Yuan-Ming Cai, and Chang-Hong Liang. "Design of electrically small metamaterial antenna with ELC and EBG loading." *IEEE Antennas and Wireless Propagation Letters* 12 (2013): 678-681. <https://doi.org/10.1109/LAWP.2013.2264099>
- [26] Xia, Yinfeng, Shengyuan Luo, and Yingsong Li. "MIMO antenna array decoupling based on a metamaterial structure." In *2018 IEEE Asia-Pacific Conference on Antennas and Propagation (APCAP)*, pp. 383-384. IEEE, 2018. <https://doi.org/10.1109/APCAP.2018.8538027>
- [27] H.Yahaya, "About 100,000 Malaysians suffer from cancer each year," *The Star* April 3, 2016.
- [28] Youssef, M. A., and A. M. M. A. Allam. "Implanted antenna on human breast." *2014 International Conference on Engineering and Technology (ICET)*. IEEE, 2014. <https://doi.org/10.1109/ICEngTechnol.2014.7016828>
- [29] Ali, Nagia, Rasime Uyguroglu, and A. M. M. A. Allam. "Cancer diagnosis in breast using biological and electromagnetic properties of breast tissues on antenna performance." In *2018 18th Mediterranean Microwave Symposium (MMS)*, pp. 325-329. IEEE, 2018. <https://doi.org/10.1109/MMS.2018.8612104>
- [30] Ali, N., MF Abo Sree, R. Uyguroglu, and A. M. M. A. Allam. "Stage II cancer diagnosis using printed antenna implemented on hemispherical model for human breast." *Journal of Instrumentation* 15, no. 09 (2020): P09016. <https://doi.org/10.1088/1748-0221/15/09/P09016>
- [31] Sree, Mohamed F. Abo, A. M. M. A. Allam, and Hesham A. Mohamed. "Design and implementation of multiband metamaterial antennas." In *2020 International Applied Computational Electromagnetics Society Symposium (ACES)*, pp. 1-2. IEEE, 2020. <https://doi.org/10.23919/ACES49320.2020.9196150>
- [32] Sree, Mohamed Fathy Abo, and A. M. M. Allam. "Design and fabrication of ultra-wideband leaky wave metamaterial antennas." *Journal of Instrumentation* 14, no. 11 (2019): P11006. <https://doi.org/10.1088/1748-0221/14/11/P11006>
- [33] Abdelghany, Mahmoud A., Mohamed Fathy Abo Sree, Arpan Desai, and Ahmed A. Ibrahim. "Gain improvement of a dual-band CPW monopole antenna for sub-6 GHz 5G applications using AMC structures." *Electronics* 11, no. 14 (2022): 2211. <https://doi.org/10.3390/electronics11142211>

- [34] Ashyap, Adel YI, Zuhairiah Zainal Abidin, Samsul Haimi Dahlan, Huda A. Majid, Muhammad Ramlee Kamarudin, and Raed A. Abd-Alhameed. "Robust low-profile electromagnetic band-gap-based on textile wearable antennas for medical application." In *2017 International Workshop on Antenna Technology: Small Antennas, Innovative Structures, and Applications (iWAT)*, pp. 158-161. IEEE, 2017. <https://doi.org/10.1109/IWAT.2017.7915346>
- [35] Ashyap, Adel YI, Zuhairiah Zainal Abidin, Samsul Haimi Dahlan, Huda A. Majid, Shaharil Mohd Shah, Muhammad Ramlee Kamarudin, and Akram Alomainy. "Compact and low-profile textile EBG-based antenna for wearable medical applications." *IEEE Antennas and Wireless Propagation Letters* 16 (2017): 2550-2553. <https://doi.org/10.1109/LAWP.2017.2732355>
- [36] Ali, N., MF Abo Sree, R. Uyuguroglu, and A. M. M. A. Allam. "Stage II cancer diagnosis using printed antenna implemented on hemispherical model for human breast." *Journal of Instrumentation* 15, no. 09 (2020): P09016. <https://doi.org/10.1088/1748-0221/15/09/P09016>
- [37] Zhong, Huiteng, and Xuexia Yang. "Broadband meta-surface with polarization-insensitive and wide-angle for electromagnetic energy harvesting." In *2017 International Workshop on Antenna Technology: Small Antennas, Innovative Structures, and Applications (iWAT)*, pp. 125-128. IEEE, 2017.
- [38] Hu, Wei, Zhao Yang, Fading Zhao, Guangjun Wen, Jian Li, Yongjun Huang, Daniele Insera, and Zhizhang Chen. "Low-cost air gap metasurface structure for high absorption efficiency energy harvesting." *International Journal of Antennas and Propagation* 2019 (2019): 1-8. <https://doi.org/10.1155/2019/1727619>
- [39] Ramahi, Omar M., Thamer S. Almoneef, Mohammed AlShareef, and Muhammed S. Boybay. "Metamaterial particles for electromagnetic energy harvesting." *Applied Physics Letters* 101, no. 17 (2012). <https://doi.org/10.1063/1.4764054>
- [40] Alavikia, Babak, Thamer S. Almoneef, and Omar M. Ramahi. "Complementary split ring resonator arrays for electromagnetic energy harvesting." *Applied Physics Letters* 107, no. 3 (2015).
- [41] Alavikia, Babak, Thamer S. Almoneef, and Omar M. Ramahi. "Wideband resonator arrays for electromagnetic energy harvesting and wireless power transfer." *Applied physics letters* 107, no. 24 (2015). <https://doi.org/10.1063/1.4927238>
- [42] Alavikia, Babak, Thamer S. Almoneef, and Omar M. Ramahi. "Wideband resonator arrays for electromagnetic energy harvesting and wireless power transfer." *Applied physics letters* 107, no. 24 (2015). <https://doi.org/10.1063/1.4937591>
- [43] Ziolkowski, Richard W., and Ehud Heyman. "Wave propagation in media having negative permittivity and permeability." *Physical review E* 64, no. 5 (2001): 056625. <https://doi.org/10.1063/1.4937591>
- [44] Rahayu, Yusnita, M. Khairon, Khairul Najmy Abdul Rani, and Teguh Praludi. "Detection of Breast Tumour Depth using Felt Substrate Textile Antenna." *Journal of Advanced Research in Applied Sciences and Engineering Technology* 39, no. 1 (2024): 59-75. <https://doi.org/10.37934/arasent.39.2.258269>
- [45] Halim, Ahmad Ashraf Abdul, Vijayarveswari Veeraperumal, Allan Melvin Andrew, Mohd Najib Mohd Yasin, Mohd Zamri Zahir Ahmad, Kabir Hossain, Bifta Sama Bari, and Fatinnabila Kamal. "UWB-based early breast cancer existence prediction using artificial intelligence for large data set." *Journal of Advanced Research in Applied Sciences and Engineering Technology* 29, no. 2 (2023): 81-90. <https://doi.org/10.37934/arasent.29.1.5975>
- [46] Zhang, Xuanming, Haixia Liu, and Long Li. "Electromagnetic power harvester using wide-angle and polarization-insensitive metasurfaces." *Applied sciences* 8, no. 4 (2018): 497. <https://doi.org/10.37934/arasent.29.2.8190>
- [47] Almoneef, Thamer S., and Omar M. Ramahi. "Metamaterial electromagnetic energy harvester with near unity efficiency." *Applied Physics Letters* 106, no. 15 (2015). <https://doi.org/10.3390/app8040497>
- [48] Ghaneizadeh, Alireza, Khalil Mafinezhad, and Mojtaba Joodaki. "Design and fabrication of a 2D-isotropic flexible ultra-thin metasurface for ambient electromagnetic energy harvesting." *AIP Advances* 9, no. 2 (2019). <https://doi.org/10.1063/1.4916232>
- [49] Duan, Xin, Xing Chen, Yonghong Zhou, Lin Zhou, and Shuji Hao. "Wideband metamaterial electromagnetic energy harvester with high capture efficiency and wide incident angle." *IEEE Antennas and Wireless Propagation Letters* 17, no. 9 (2018): 1617-1621. <https://doi.org/10.1063/1.5083876>
- [50] Yu, Fan, Xuexia Yang, Huiteng Zhong, Chengyi Chu, and Steven Gao. "Polarization-insensitive wide-angle-reception metasurface with simplified structure for harvesting electromagnetic energy." *Applied physics letters* 113, no. 12 (2018). <https://doi.org/10.1109/LAWP.2018.2858195>
- [51] Ghaderi, Bagher, Vahid Nayyeri, Mohammad Soleimani, and Omar M. Ramahi. "Pixelated metasurface for dual-band and multi-polarization electromagnetic energy harvesting." *Scientific reports* 8, no. 1 (2018): 13227. <https://doi.org/10.1063/1.5046927>
- [52] Zhang, Xuanming, Haixia Liu, and Long Li. "Tri-band miniaturized wide-angle and polarization-insensitive metasurface for ambient energy harvesting." *Applied physics letters* 111, no. 7 (2017). <https://doi.org/10.1038/s41598-018-31661-6>

- [52] Zhong, Hui-Teng, Xue-Xia Yang, Xing-Tang Song, Zhen-Yue Guo, and Fan Yu. "Wideband metamaterial array with polarization-independent and wide incident angle for harvesting ambient electromagnetic energy and wireless power transfer." *Applied physics letters* 111, no. 21 (2017). <https://doi.org/10.1063/1.4999327>
- [53] Zhong, Hui-Teng, Xue-Xia Yang, Chong Tan, and Kai Yu. "Triple-band polarization-insensitive and wide-angle metamaterial array for electromagnetic energy harvesting." *Applied physics letters* 109, no. 25 (2016). <https://doi.org/10.1063/1.4973282>